

Solution Structure Model of Residues 1–28 of the Amyloid β -Peptide When Bound to Micelles

Keith J. Marcinowski, Haiyan Shao, Erin L. Clancy, and Michael G. Zagorski*

Contribution from the Department of Chemistry, Case Western Reserve University, Cleveland, Ohio 44106

Received November 11, 1997. Revised Manuscript Received July 7, 1998

Abstract: The major protein constituent of amyloid deposits in Alzheimer's disease is the β -peptide, which in solution can fold as a random coil, monomeric α -helix, or oligomeric β -sheet structure, the latter structure being toxic and eventually precipitating as amyloid. In this report, using circular dichroism and nuclear magnetic resonance spectroscopic techniques, we demonstrate that in micelle solution the α -helical structure is the predominate structural motif and that its stability is highly dependent on the pH and the surface charge of the micelle. A peptide fragment comprised of residues 1–28 of the β -peptide [β -(1–28)], which occupies the presumed extracellular domain of the amyloid precursor protein and the negatively charged sodium dodecyl sulfate (SDS), the positively charged dodecyltrimethylammonium chloride (DTAC), and the zwitterionic, neutral dodecylphosphocholine (DPC), was utilized. In SDS and DPC, nuclear Overhauser enhancement spectroscopy and the α H chemical shifts showed that at pH 2–3 there are two α -helical regions located within the Ala2–Asp7 and Tyr10–Lys28 peptide regions. Temperature coefficients for the amide-NH established that the 1–28 region is located at the micelle surface and does not insert into the hydrophobic interior. Above pH 4, no α -helix forms in DPC, whereas the Tyr10–Lys28 helix remained α -helical in SDS up to pH 9.5. With DTAC, the α -helix formed at high pH, and below pH 4 only random coil was present. Most importantly, the present data demonstrate that micelles prevent formation of the toxic β -sheet structure for the 1–28 region, which may eventually have therapeutic implications for the treatment of Alzheimer's disease.

Introduction

Alzheimer's disease (AD) is characterized by an abundance of amyloid deposits that contain the β -peptide, a small (39–43 amino acids) peptide with heterogeneous termini that is generated from cleavage of a larger amyloid precursor protein (APP).^{1,2} Extracellular amyloid plaque core is primarily composed of the β -(1–42), while cerebrovascular amyloid contains the more soluble β -(1–39) and β -(1–40) peptides (Figure 1). The β -(1–28) and β -(29–42) peptides, which are composed of amino acid residues 1–28 and 29–42, occupy the extracellular and transmembrane domains within APP.

The β -peptide is ubiquitous in the biological fluids of humans.^{3–6} Because individuals with or without AD have comparable amounts of soluble β -peptide in plasma and cerebrospinal fluid,^{4,7} a distinguishing feature is the presence of larger amounts of the insoluble (amyloid) form in the brains

Asp¹-Ala²-Glu³-Phe⁴-Arg⁵-His⁶-Asp⁷-Ser⁸-Gly⁹-Tyr¹⁰-Glu¹¹-Val¹²-His¹³-His¹⁴-Gln¹⁵-Lys¹⁶-Leu¹⁷-Val¹⁸-Phe¹⁹-Phe²⁰-Ala²¹-Glu²²-Asp²³-Val²⁴-Gly²⁵-Ser²⁶-Asn²⁷-Lys²⁸-Gly²⁹-Ala³⁰-Ile³¹-Ile³²-Gly³³-Leu³⁴-Met³⁵-Val³⁶-Gly³⁷-Gly³⁸-Val³⁹-Val⁴⁰-Ile⁴¹-Ala⁴²

Figure 1. Amino acid sequence of the amyloid β -(1–42) peptide, with the β -(1–28) peptide region occupying residues 1–28. To exemplify the amphipathicity, the charged and noncharged, polar residues are shown in bold and underlined, respectively.

of AD patients. In vitro studies^{8–12} indicate that synthetic β -peptides can adopt random coil, monomeric α -helical, or oligomeric β -sheet conformations in solution. The α -helical conformation is very soluble, whereas the β -sheet conformation is oligomeric and neurotoxic and eventually precipitates as an amyloid.¹³ At low and high pH, the β -(1–28) is mostly unstructured in aqueous solution but becomes α -helical in membrane mimetic environments such as trifluoroethanol (TFE). At pH 4–7 the peptide rapidly produces an aggregated β -sheet structure in water with or without TFE.

* To whom correspondence should be addressed. Telephone: 216-368-3706. Fax: 216-368-3006. E-mail: mxz12@po.cwru.edu.

- (1) Selkoe, D. J. *Annu. Rev. Neurosci.* **1994**, *17*, 489–517.
- (2) Iqbal, K.; Winblad, B.; Nishimura, T.; Takeda, M.; Wisniewski, H. M. *Alzheimer's Disease: Biology, Diagnosis, and Therapeutics*; Iqbal, K., Winblad, B., Nishimura, T., Takeda, M., Wisniewski, H. M., Eds.; John Wiley & Sons, Ltd.: New York, 1997.
- (3) Haass, C.; Schlossmacher, M. G.; Hung, A. Y.; Vigo-Pelfrey, C.; Mellon, A.; Ostaszewski, B. L.; Lieberburg, I.; Koo, E. H.; Schenk, D.; Teplow, D. B.; Selkoe, D. J. *Nature* **1992**, *359*, 322–325.
- (4) Shoji, M.; Golde, T. E.; Cheung, T.; Ghiso, J.; Estus, S.; Shaffer, L. M. *Science* **1992**, *258*, 126–129.
- (5) Seubert, P.; Vigo-Pelfrey, C.; Esch, F.; Lee, M.; Dovey, H.; Davis, D.; Sinha, S.; Schlossmacher, M.; Whaley, J.; Swindlehurst, C.; McCormack, R.; Wolfert, R.; Selkoe, L. I.; Schenk, D. *Nature* **1992**, *359*, 325–327.
- (6) Busciglio, J.; Gabuzda, D. H.; Matsudaira, P.; Yanker, B. A. *Proc. Natl. Acad. Sci. U.S.A.* **1993**, *90*, 2092–2096.

- (7) Southwick, P. C.; Yamagata, S. K.; Echols, C. L.; Higson, G. J.; Neynaber, S. A.; Parson, R. e.; Munroe, W. A. *J. Neurochem.* **1996**, *66*, 259–265.
- (8) Barrow, C. J.; Zagorski, M. G. *Science* **1991**, *253*, 179–182.
- (9) Fraser, P. E.; Nguyen, J. T.; Surewicz, W. K.; Kirschner, D. A. *Biophys. J.* **1991**, *60*, 1190–1201.
- (10) Hilbich, C.; Kisters-woide, B.; Reed, J.; Masters, C. L.; Beyreuther, K. *J. Mol. Biol.* **1991**, *218*, 149–163.
- (11) Burdick, D.; Soreghan, B.; Kwon, M.; Kosmoski, J.; Knauer, M.; Henschen, A.; Yates, J.; Cotman, C.; Glabe, C. *J. Biol. Chem.* **1992**, *267*, 546–554.
- (12) Otvos, L. J.; Szendrei, G. I.; Lee, V. M. Y.; Mantsch, H. H. *Eur. J. Biochem.* **1993**, *211*, 249–257.
- (13) Iversen, L. L.; Mortishire-Smith, R. J.; Pollack, S. J.; Shearman, M. S. *Biochem. J.* **1995**, *311*, 1–16.

Although the β -(1–28) peptide does not bind to pre-existing amyloid plaques,¹⁴ it is an appropriate structural model for the complete β -(1–42) peptide, since it produces soluble monomeric α -helical structures,^{8,12} as well as plaque-like oligomeric β -sheet structures, similar to those found in natural amyloid plaques.^{15,16} In fact, it has been proposed that the α -helix in the 1–28 region is critical to normal α -secretase cleavage of APP, which generates non-amyloidogenic APP fragments.¹⁷ The hydrophobic 29–42 region increases the rate of aggregation and β -sheet production and probably also accounts for its attachment to pre-existing amyloid plaques.^{10,11,18,19} Notwithstanding over a decade of research efforts aimed at preventing amyloid formation in AD, the mechanisms in which the β -peptide self-assembles in vivo into amyloid remain unknown.

Numerous studies have documented the importance of β -peptide/lipid interactions in AD. In plasma or cerebrospinal fluid, the β -peptide binds to various hydrophobic macromolecules such as apolipoproteins (Apo-E and Apo-J), high-density lipoproteins (HDL), albumin, transthyretin, proteasomes, and other lipoproteins, which may have implications for the circulation of the β -peptide in biological fluids.^{20–24} Other research has shown that interactions of the β -peptides with lipid bilayers or neuronal membranes can increase both the fluidity and intracellular calcium levels, produce voltage-dependent ion channels, and exert other effects such as blockage and excitability on potassium channels.^{25–29} These processes, along with the aggregation into β -sheet structures,^{30,31} are thought to be involved in the β -peptide-induced neurotoxicity. Together, these results demonstrate that the aggregation state and structure of the β -peptide in membrane-like environments are important pathological events in AD.

To provide a molecular basis for the role of biological membranes in amyloid formation, the solution structures of the β -(1–28) peptide in detergent micelles was investigated using

CD and NMR as complimentary spectroscopic techniques. The approach of using micelles such as sodium dodecyl sulfate (SDS) and dodecylphosphocholine (DPC) to mimic the molecular environment of biological membranes has been successfully applied to many peptides and proteins.^{32–34} Micelles from the negatively charged SDS, neutral DPC, and positively charged DTAC detergents were used as membrane models. Some of these results were reported by us earlier,^{35,36} and the present work represents a more comprehensive study that demonstrates that the micelle charge and solution pH have profound outcomes in promoting structure. The α -helix is stabilized over a wide pH range in the charged SDS and DTAC micelles, whereas with the zwitterionic, neutral DPC micelle, the α -helix exists only below pH 4. The present work also establishes that the β -(1–28) associates on the micelle surface, consistent with its location in the extracellular region of the APP. The implications of these data to the binding of the β -peptide to biological lipids and amyloid formation are discussed.

Results

Circular Dichroism Studies. The CD spectra for the β -(1–28) peptide in SDS, DPC, and DTAC solutions are shown in Figure 2. Spectra were obtained at pH values ranging from approximately 2 to 11. Within this pH range, the SDS, DPC, and DTAC micelles retain their net negative, neutral, and positive charges, respectively, since their pK_a values are well below 1.^{37,38} The CD spectra establish that there are two predominant conformations, random coil and α -helix. Typically, spectra for the α -helix have a strong positive band at 195 nm and two, intense negative bands at 208 and 222 nm, while the random coil is characterized by a strong negative band at 198 nm.^{39,40} No discernible β -sheet structure was detected in any of the micelle solutions, which would be noticed by a distinct broad negative band at 217 nm. The isodichroic points at approximately 205 nm, which is a region where all CD traces converge, demonstrate that two conformations, the α -helix and random coil, coexist in solution.

In SDS, the β -(1–28) peptide adopts predominately α -helix (Figure 2A), which remains somewhat constant at approximately 75–85 and 50–65% within two pH ranges, pHs 3.0–5.0 and 5.8–9.5, respectively (Table 1). At pHs 10.9 and 11.8, the peptide becomes random coil, as demonstrated by the intense negative band at 198 nm.

With the zwitterionic, neutral DPC micelle, little α -helix forms above pH 4.4 (Figure 2B), in which the α -helical content drops to 10–20% with the major conformation being random coil. At acidic pH, however, the CD data in SDS and DPC are very similar, showing about 85% α -helix (Table 1). In 60% TFE, approximately 85% α -helix also forms at low pH, which together indicates a greater helical propensity at acidic pH.¹⁸

- (14) Maggio, J. E.; Mantyh, P. W. *Brain Pathol.* **1996**, *6*, 147–162.
 (15) Gorévic, P. D.; Castano, E. M.; Sarma, R.; Frangione, B. *Biochem. Biophys. Res. Commun.* **1987**, *147*, 854–862.
 (16) Kirschner, D. A.; Inouye, H.; Duffy, L. K.; Sinclair, A.; Lind, M.; Selkoe, D. J. *Proc. Natl. Acad. Sci. U.S.A.* **1987**, *84*, 6953–6957.
 (17) Sisodia, S. S. *Proc. Natl. Acad. Sci. U.S.A.* **1992**, *89*, 6075–6079.
 (18) Barrow, C. J.; Yasuda, A.; Kenny, P. T. M.; Zagorski, M. G. *J. Mol. Biol.* **1992**, *225*, 1075–1093.
 (19) Jarrett, J. T.; Beger, E. P.; Lansbury, P. T. *Biochemistry* **1993**, *32*, 4693–4697.
 (20) Schwarzman, A. L.; Gregori, L.; Vitek, M. P.; Lyubski, S.; Strittmatter, W. J.; Enghilde, J. J.; Bhasin, R.; Silverman, J.; Weisgraber, K. H.; Coyle, P. K.; Zagorski, M. G.; Talafous, J.; Eisenberg, M.; Saunders, A. M.; Roses, A. D.; Goldgaber, D. *Proc. Natl. Acad. Sci.* **1994**, *91*, 8368–8372.
 (21) Roses, A. D. *J. NIH Res.* **1995**, *7*, 51–56.
 (22) Koudinov, A. R.; Koudinova, N. V.; Kumar, A.; Beavis, R. C.; Ghiso, J. *Biochem. Biophys. Res. Commun.* **1996**, *223*, 592–597.
 (23) Matsubara, E.; Soto, C.; Governale, S.; Frangione, B.; Ghiso, J. *Biochem. J.* **1996**, *316*, 671–679.
 (24) Biere, A. L.; Ostaszewski, B.; Stimson, E. R.; Hyman, B. T.; Maggio, J. E.; Selkoe, D. J. *J. Biol. Chem.* **1996**, *271*, 32916–32922.
 (25) Arispe, N.; Pollard, H. B.; Rojas, E. *Proc. Natl. Acad. Sci. U.S.A.* **1993**, *90*, 10573–10577.
 (26) Mattson, M. P.; Tomaselli, K. J.; Rydel, R. E. *Brain Res.* **1993**, *621*, 35–49.
 (27) Good, T. A.; Murphy, R. M. *Proc. Natl. Acad. Sci.* **1996**, *93*, 15130–15135.
 (28) Kawahara, M.; Arispe, N.; Kuroda, Y.; Rojas, E. *Biophysical J.* **1997**, *73*, 67–75.
 (29) Avdulov, N.; Chochina, S. V.; Igbavboa, U.; O'Hare, E. O.; Schroeder, F.; Cleary, J. P.; Wood, W. G. *J. Neurochem.* **1997**, *68*, 2086–2091.
 (30) Simmons, L. K.; May, P. C.; Tomaselli, K. J.; Rydel, R. E.; Fuson, K. S.; Brigham, E. F.; Wright, S.; Lieberburg, L.; Becker, G. W.; Brems, D. N.; Li, W. *Mol. Pharmacol.* **1994**, *45*, 373–379.
 (31) Pike, C. J.; Walencewicz-Wasserman, A. J.; Kosmoski, J.; Cribbs, D. H.; Glabe, C. G.; Cotman, C. W. *J. Neurochem.* **1995**, *64*, 253–265.

- (32) McDonnell, P. A.; Opella, S. J. *J. Magn. Reson. B* **1993**, *102*.
 (33) Henry, G. D.; Sykes, B. D. *Methods Enzymol.* **1994**, *239*, 520–534.
 (34) Opella, S. J. *Nat. Struct. Biol.* **1997**, *4*, 845–848.
 (35) Talafous, J.; Marcinowski, K. J.; Klopman, G.; Zagorski, M. G. *Biochemistry* **1994**, *33*, 7788–7796.
 (36) Shao, H.; Marcinowski, K. J.; Clancy, E. L.; Salomon, A. R.; Zagorski, M. G. *The Solution Structures of the β -Amyloid Peptide Provide a Molecular Approach for the Treatment of Alzheimer's Disease*; Shao, H., Marcinowski, K. J., Clancy, E. L., Salomon, A. R., Zagorski, M. G., Eds.; John Wiley & Sons, Ltd.: New York, 1997; pp 729–739.
 (37) Tanford, C. *The Hydrophobic Effect: Formation of Micelles and Biological Membranes*; Wiley: New York, 1973.
 (38) Chupin, V.; Killian, J. A.; Breg, J.; de Jongh, H. H. J.; Boelens, R.; Kaptein, R.; Kruijff, B. *Biochemistry* **1995**, *34*, 11617–11624.
 (39) Greenfield, N.; Fasman, G. D. *Biochemistry* **1969**, *8*, 4108–4116.
 (40) Woody, R. W. *Circular Dichroism of Peptides and Proteins*; VCH Publishers: New York, 1994.

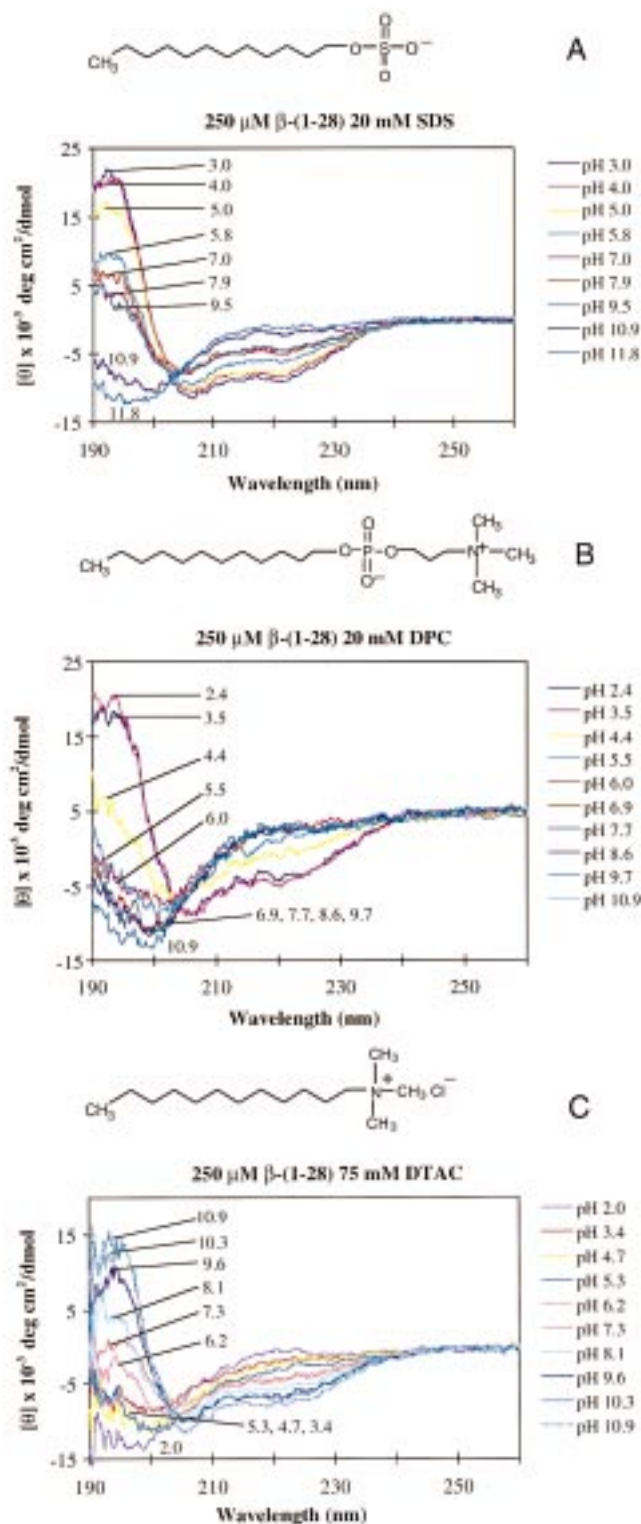


Figure 2. CD spectra for the β -(1–28) (250 μ M) in aqueous solution containing three different micelles: the negatively charged sodium dodecyl sulfate (SDS) (A), neutral dodecylphosphocholine (DPC) (B), and positively charged dodecyltrimethylammonium chloride (DTAC) (C). The chemical structures of the micelles in monomeric form are provided above the CD data. Spectra obtained at different pH values are color-coded for a particular pH and labeled within the figure. The spectra demonstrate the sensitivity of conformation with pH, with the α -helix favored at low and midrange pH in SDS, low pH in DPC, and high pH in DTAC solutions. The percent α -helix for each pH are summarized in Table 1. The presence of isodichroic points demonstrate that two conformations (α -helix and random coil) coexist in solution.

Table 1. Effect of pH on the Percentage of α -Helical Structure for the β -(1–28) Peptide in DTAC, DPC, and SDS Micelle Solutions^a

DTAC		DPC		SDS	
pH	% helix	pH	% helix	pH	% helix
2.0	0	2.4	85	3.0	85
3.4	10	3.5	80	4.0	85
4.7	5	4.4	20	5.0	75
5.3	10	5.0	15	5.8	65
6.2	20	6.0	10	7.0	55
7.3	35	6.9	5	7.9	55
8.1	60	7.7	5	9.5	50
9.6	75	8.6	5	10.9	10
10.3	85	9.7	0	11.8	0
10.9	85	10.9	0		

The data at midrange pH (4–7) and neutral pHs suggest that SDS is more hydrophobic and α -helix promoting than DPC, consistent with CD and NMR studies of prion protein fragments.⁴¹

Interaction of the β -(1–28) peptide with the positively charged DTAC micelle showed predominantly random coil structure at low pH and α -helix at high pH (Figure 2C). This pattern is opposite to that seen in SDS, except that slightly more helix exists in SDS at neutral pH (Table 1). The α -helical content at pH 3.0–3.5 was estimated to be 10, 80, and 85% in DTAC, DPC, and SDS solutions, respectively (Table 1).

Identical secondary structure estimates were obtained within the peptide concentration range 1.0–0.02 mM, thus establishing that the α -helical structure is monomeric. Additionally, identical results were obtained at 20 and 75 mM micelle concentrations, which are both well above the critical micelle concentrations for SDS and DPC.^{33,42}

At low and high pH, in aqueous solutions without micelles, the β -(1–28) is predominantly random coil, although at pH 4–7 β -sheet structure forms.^{9,18,43} In 60% TFE, the α -helix forms at low and high pHs, similar to the present data, whereas at pH 4–7, an irreversible α -helix (monomeric) \rightarrow β -sheet (oligomeric) conversion occurs. These studies establish that membrane-like media with a charged surface are more effective in stabilizing the soluble α -helical conformation of the β -peptide in the physiological pH range and prevent aggregation into the β -sheet. For all micelle solutions, the conformations were stable and reproducible over the complete pH range. The samples remained clear and no peptide precipitation took place, which suggests amenable systems for solution NMR studies.

NMR Studies. To specifically locate the α -helical and random coil regions in the primary sequence, the β -(1–28) was further studied by ¹H NMR. Both SDS and DPC have relatively small sizes that undergo rapid isotropic motions, thus enabling high-resolution NMR spectra to be obtained. In addition, these micelles are commercially available in perdeuterated forms (DPC-*d*₃₈ and SDS-*d*₂₅), which eliminates their ¹H resonances and overcomes problems of possible NOE spin diffusion effects within the micelle. Since the CD data showed maximum α -helix formation at acidic pH, the NMR studies were initially performed below pH 3. These studies would establish whether the same peptide regions become helical in SDS and DPC.

With the exception of minor chemical shift differences for some residues at the N-terminus, 1D ¹H NMR spectra obtained

(41) Zhang, H.; Kaneko, K.; Nguyen, J. T.; Livshits, T. L.; Baldwin, M. A.; Cohen, F. E.; James, T.; Prusiner, S. B. *J. Mol. Biol.* **1995**, *250*, 514–526.

(42) Lauterwein, J.; Bösch, C.; Brown, L.; Wüthrich, K. *Biochim. Biophys. Acta* **1979**, *556*, 244–264.

(43) Good, T. A.; Murphy, R. M. *Biochem. Biophys. Res. Commun.* **1995**, *207*, 209–215.

in SDS or DPC at β -(1–28) concentrations of 0.41 mM were virtually identical to those obtained at 2.0 mM. The lack of any concentration-dependent changes in the chemical shifts supports the presence of monomeric structure for the β -(1–28).⁴⁴ In addition, there were no significant changes in chemical shifts with alterations of the micelle/peptide ratio, thus showing that the occurrence of one peptide molecule per micelle does not influence the secondary structure.^{32,33}

To further address the issue of aggregation, we measured the diffusion coefficients (D) of the β -(1–28) in SDS solution at two different peptide concentrations, using well-established pulse field gradient (PFG) techniques.⁴⁵ The D provides reliable information about the molecular sizes and the apparent molecular weights of proteins and, in some cases, can also provide fractional populations of different oligomeric states.⁴⁶ For the β -(1–28), the D values were obtained by monitoring signal losses in the upfield methyl and downfield aromatic spectral regions as a function of gradient strength. At 0.2 and 2.0 mM β -(1–28) concentrations, the overall D values (micelle and peptide) were 6.1×10^{-7} and 6.3×10^{-7} cm² s⁻¹, respectively. These values are experimentally indistinguishable and are within the precision of our measurements ($\pm 0.24 \times 10^{-7}$ cm² s⁻¹), as determined by performing the measurements in triplicate. Altogether, the diffusion measurements, along with the data obtained in the 1D NMR and CD concentration studies (previous paragraph), establish that within the 0.2–2.0 mM concentration range the aggregation state is constant and compatible with a monomeric structure.

Shown in Figure S1 is the complete 2D nuclear Overhauser enhancement spectroscopy (NOESY) spectrum (250-ms mixing time) in DPC solution. Spectra acquired with shorter mixing times had identical but weaker cross-peak intensities, indicating that spin diffusion was negligible. The presence of numerous, well-resolved cross-peaks indicates that the peptide is folded and that assignments should be possible using standard homonuclear NMR methods. The well-established sequential assignment protocol was used to assign the complete ¹H NMR spectra of the β -(1–28) in SDS and DPC.^{47–50} Two experiments were utilized to complete the assignments: (1) the total correlation spectroscopy (TOCSY) experiment that provides through-bond, direct (two- or three-bond), and relayed connectivity (greater than three bonds) and (2) the NOESY experiment that provides through-space connections. The TOCSY spectra (not shown) were used to identify spin systems, while the NOESY spectra were used to obtain inter-residue connectivities and an accurate estimation of the secondary structure. Another NMR parameter for the identification and location of secondary structures comes from the backbone J -coupling constant data. Unfortunately, due to the increased line widths in the micelle solutions, coupling constants could not be measured from standard COSY experiments.

An expanded region of the NOESY spectrum in DPC is shown in Figure 3. This spectrum demonstrates numerous sequential NH(i) to NH($i+1$) NOEs [NN($i,i+1$)] between adjacent amide-NH protons, which is diagnostic for α -helices.

(44) Lee, J. P.; Stimson, E. R.; Ghilardi, J. R.; Mantyh, P. W.; Lu, Y.-A.; Felix, A. M.; Llanos, W.; Behbin, A.; Cummings, M.; van Criekinge, M.; Timms, W.; Maggio, J. E. *Biochemistry* **1995**, *34*, 5191–5200.

(45) Altieri, A. S.; Hinton, D. P.; Byrd, R. A. *J. Am. Chem. Soc.* **1995**, *117*, 7566–7567.

(46) Mayo, K. H.; Ilyina, E. *Protein Sci.* **1998**, *7*, 358–368.

(47) Wüthrich, K. *NMR of Proteins and Nucleic Acids*; Wiley: New York, 1986.

(48) Gronenborn, A. M.; Clore, M. G. *Anal. Chem.* **1990**, *62*, 2–15.

(49) Case, D. A.; Wright, P. E. *Determination of High-Resolution NMR Structures of Proteins*; CRC: Ann Arbor, MI, 1993.

(50) Bax, A.; Grzesiek, S. *Acc. Chem. Res.* **1993**, *26*, 131–138.

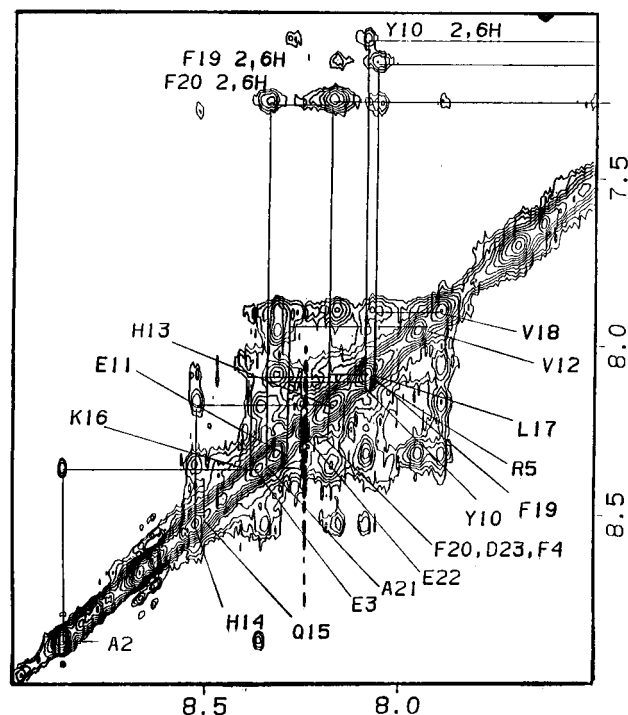


Figure 3. Expanded 2D NOESY showing numerous amide–amide (NH–NH) connectivities. Intra- and inter-residue NOE interactions between the aromatic 2,6Hs of Tyr10 and the NH of both Tyr10 and Glu11, as well as between the 2,6Hs of Phe19 and Phe20 to the NHs of Phe19, Phe20, and Ala21 are shown. Data were processed on a Silicon Graphics Indigo computer using the FELIX program (version 95.0, Biosym, Inc.).

Additional inter- and intra-residue NOEs from the aromatic ring protons of Tyr10, Phe19, and Phe20 are also shown. Analysis of the NOESY data in other regions showed numerous medium-range α N($i,i+2$), α N($i,i+3$), and α B($i,i+3$) NOEs, which are likewise consistent with a predominantly α -helical structure, in accordance with the CD data (Table 1). A complete listing of the inter-residue NOEs in SDS and DPC is shown in Figure 4, and the complete ¹H NMR assignments are provided in Tables SI and SII.

Most of the α H signals appear upfield relative to random coil shift values, indicative of α -helical structure.⁵¹ The NOE data in SDS and DPC are very similar (Figure 4), as well as with previous data obtained in 60% TFE.⁵² The major differences are in the Tyr10–Val18 region, in which there are four α N($i,i+2$) NOEs in DPC compared to only one in SDS. This suggests that a shorter α -helix or possibly 3_{10} -helix may be present in DPC. However, the presence of two α N($i,i+4$) NOEs indicates that a 3_{10} -helix is not likely present, although it may exist as a minor species in the conformational ensemble. Further inspection of the NOE data suggests that in SDS and DPC there are two α -helical segments, Ala2–Asp7 and Tyr10–Lys28, with the Ser8–Gly9 region serving as a connecting segment between the two helices. There are differences in the stabilities of the two helical regions, in that the Ala2–Asp7 helix has a greater tendency to unfold into a random coil structure, as previously seen in 60% TFE.⁵² The number of α -helical NOE connectivities and their intensities are greater for the Tyr10–Lys28 helix, particularly with the medium-range α N($i,i+3$) and α B($i,i+3$) NOEs (Figure 4).

(51) Wishart, D. S.; Sykes, B. D.; Richards, F. M. *Biochemistry* **1992**, *31*, 1647–1651.

(52) Zagorski, M. G.; Barrow, C. J. *Biochemistry* **1992**, *31*, 5621–5631.

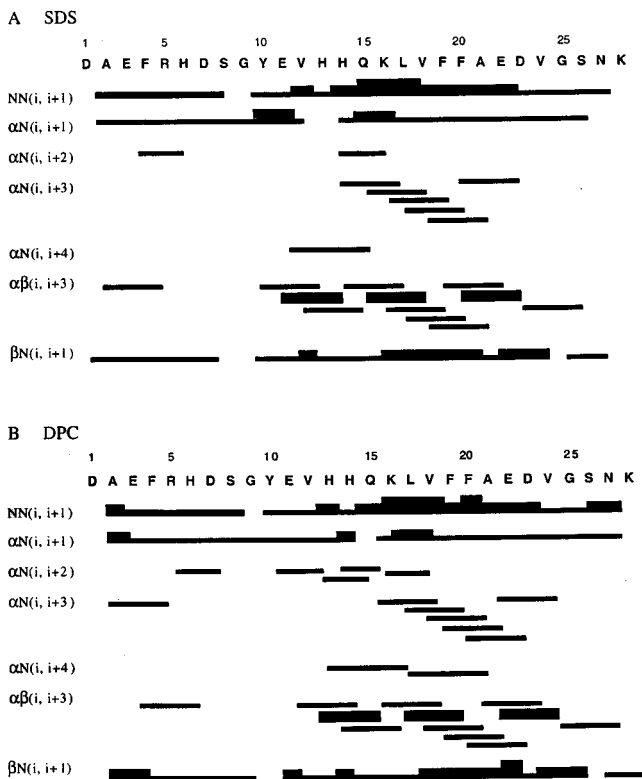


Figure 4. Summary of the observed inter-residue NOE connectivities for the β -(1–28) in water (9:1, H₂O:D₂O) containing SDS-*d*₂₅ (A) and DPC-*d*₃₈ (B). The complete assignments and conditions are provided in Supporting Information Tables SI and SII. The thickness of the horizontal bars corresponds approximately to the size of the NOE intensities. These data are nearly identical to previous results seen in 60% TFE solution,⁵² compatible with a tertiary structure consisting of an α -helix (Ala2–Asp7), hinge (Ser8–Gly9), and α -helix (Tyr10–Lys28).³⁵

The NMR experiments were not conducted in DPC solution above pH 5, since the CD data showed primarily random coil structure (Table 1). However, above pH 5 in SDS, nearly identical inter-residue NOEs were seen within the Tyr10–Lys28 segment, while those for the Asp1–Gly9 region mostly disappeared. This observation is consistent with a disordered structure at Asp1–Gly9 and retention of the α -helix at Tyr10–Lys28 at pH 5–8. These latter results are also consistent with the CD data, which showed both random coil and α -helix in SDS at midrange pH values (Table 1).

There were notable differences in the stabilities of the α -helices with temperature. Above 35 °C, in DPC solution, NOE cross-peaks were barely detectable, and below 15 °C, the amide-NH signals became too broad for reliable signal detection. At 40 °C in DPC, the β -(1–28) peptide became completely unfolded as a random coil structure. This was apparent from the degeneracy of many signals such as the Ala2 and Ala21 methyls, the appearance of narrow line widths and a reduction of the amide-NH chemical shift range to 0.79 ppm compared to 0.98 ppm at 20 °C. The α -helical structure was restored with reductions in temperature, indicating that α -helix (lower temperature) and random coil (higher temperature) coexist in DPC solution. By comparison, in SDS, nearly identical NOE data were seen at 25 and 50 °C, which indicates that the negatively charged SDS stabilizes the α -helix and prevents an α -helix \rightarrow random coil interconversion at higher temperatures. The changes seen with DPC are not due to a possible denaturing effect, since it is well-known that the micelle aggregation state and size are stable at elevated temperatures.³⁷

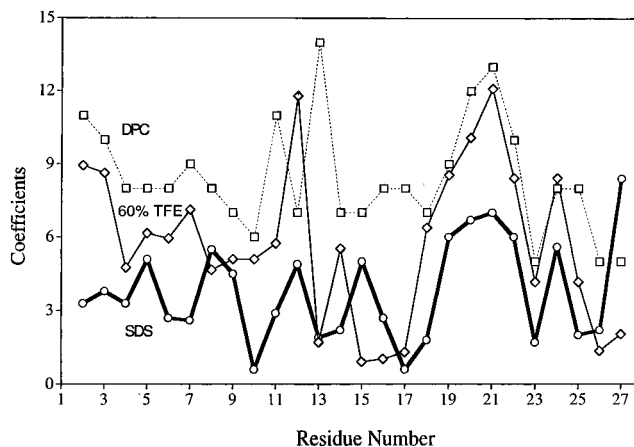


Figure 5. Graphical plot of the primary sequence against amide-NH temperature coefficients for NMR data (pH 2.5–3.0) in DPC (dotted line, squares), 60% TFE (single line, diamonds),⁵² and SDS (bold line, circles). The random pattern of the coefficients establish that the β -(1–28) peptide is located at the surface of the SDS and DPC micelles and that the negatively charged SDS micelle is most effective in stabilizing the α -helical structure. By contrast, the α -helical structure unfolds rapidly with the neutral DPC micelle. The coefficients in DPC and 60% TFE were obtained from NMR data over 15–35 °C, while those in SDS were 15–50 °C.

To further investigate the role of temperature on α -helical stability, the temperature coefficients for the amide-NH protons were determined.⁴⁷ It was not possible to obtain amide-NH exchange rates with ²H₂O solvent, since they were too rapid to be measured by fast-2D NMR methods. Also, extensive signal overlap prevented utilization of 1D NMR for the exchange measurements. The temperature dependence of the amide-NH chemical shifts is a relatively reliable indicator of hydrogen bond strength and shielding from the solvent. In general, a coefficient of less than 5 is indicative of a solvent-shielded amide-NH. Using TOCSY and NOESY data, the chemical shifts for the amide-NH peaks were obtained in SDS and DPC over 15–40 and 15–50 °C ranges, respectively. The coefficients are plotted in Figure 5, and for comparison, those in 60% TFE are also included in the graph.⁵² The magnitude of the coefficients are quite different in SDS and DPC, with much lower values seen in SDS. This observation is consistent with the retention of NOEs in SDS at 50 °C. This majority of the coefficients in DPC are greater than 5, which, together with the loss of NOEs above 35 °C, establishes that the neutral DPC micelle is less effective in stabilizing the α -helix. The most significant differences in coefficients occur within the Tyr10–His13 region, where there is a 12 ppb/°C difference in the coefficients for His13 in SDS and DPC and about 7 ppb/°C difference for Val12 in 60% TFE and SDS. For all conditions, the coefficients for the His14–Val18 region are low, indicating that these amides are the most shielded from solvent and this represents a stable region of the α -helix. Interestingly, the Phe19–Phe20–Ala21–Glu22 region has the largest coefficients in all three solvent systems, suggesting that this segment may unfold first at elevated temperature. The random pattern of coefficients, together with extremely rapid exchange rates in ²H₂O solvent, suggests that no peptide region is located within the hydrophobic interior of the SDS or DPC micelles.

Discussion

A major aim of our research is to unravel the molecular mechanisms of β -amyloidosis. More specifically, we focus at

elucidating the environmental variables that favor production of the non-amyloidogenic α -helical structure. In previous studies, we and others have showed that the predominance of a particular solution structure is highly dependent on the solvent hydrophobicity, pH, ionic strength, and peptide concentration.^{8–12,53–59} Detailed knowledge of these factors may later guide the development of suitable therapeutic approaches to prevent a related α -helix (soluble, monomeric) \rightarrow β -sheet (soluble, aggregated, toxic) \rightarrow β -sheet (insoluble, toxic, amyloid deposit) from occurring in AD.

The purpose of the present study was to examine the effects of membrane mimetic environments on the solution structures and aggregational properties of residues 1–28 of the β -peptide. It is well documented that the β -peptide becomes localized in membrane-like or lipid-rich regions in the brain, which includes binding to lipoproteins or other hydrophobic macromolecules. The SDS, DPC, and DTAC micelles provide a heterogeneous amphiphilic environment that adequately mimics a biological membrane surface.^{32–34} Thus, the micelles are systems amenable to biophysical studies of peptides and are particularly applicable for solution NMR techniques.

Effects of pH, Temperature, and Micelle Charge on the Stability of α -Helical Structure. Due to the conformational sensitivity of the β -peptide to solution conditions, before starting NMR measurements, we first conducted thorough CD studies. This enabled us to explore rapidly the influence of variables such as the pH and micelle concentrations on the secondary structures. The CD results establish that α -helix formation is strongly dependent on the pH and the surface charge of the micelle. In general, micelles with charged surfaces favor helix production, particularly the negatively charged SDS. Outlined in Figure 6 is a model for the interaction of the β -(1–28) peptide with the SDS, DPC, and DTAC micelles at pHs 1–3, 4–8, and 9–12. This mechanism takes into account the importance of electrostatic interactions for the binding between the α -helix and the micelles. The location of the peptide at the micelle surface, rather than the hydrophobic interior, is consistent with the amide-NH temperature coefficients and the rapid deuterium exchange rates, and this is further discussed in the next section.

Below pH 3, the nearly identical CD and NOE data in DPC or SDS suggest that similar α -helical structures are present (Figure 6). The NOE data show numerous sequential NN($i,i+1$) and medium-range α N($i,i+3$) and α β ($i,i+3$) NOE connectivities, characteristic for α -helices (Figure 4). The NOE data support a structure composed of two α -helices involving residues Ala2–Asp7 and Tyr10–Lys28, similar to the secondary structure obtained in 60% TFE.^{35,52}

Above pH 4, the α -helix unfolds in DPC solution to generate random coil structure (Figure 6C), whereas in SDS, residues 1–9 adopt an extended chain and the Tyr10–Lys28 region remains α -helical (Figure 6A). This latter α -helix breaks down above pH 9.5, generating completely random coil peptide. Within the physiological pH range (pH 7.2–7.6), the α -helix is stabilized with either SDS or DTAC.

The variation of structure with pH is related to α -helix unfolding and refolding (α -helix \leftrightarrow random coil) and must be related to the presence of ionizable groups. One possibility to account for the greater helical stability is that the α -helix dipole of the Tyr10–Lys28 region interacts favorably with negatively or positively charged groups of SDS or DTAC.⁶⁰ Another possibility is that electrostatic interactions affect α -helix stability. As shown in Figure 6, at pH 3–5, the side chain groups of Asp1, Glu3, Asp7, Glu11, Glu22, and Asp23 deprotonate (COOH \rightarrow COO[−]), and at pH 6–8, deprotonation of the His6, His13, and His14 side chains (3NH⁺ \rightarrow 3N) takes place.^{61,62} When protonated, the His side chains bind tighter to the negatively charged SDS and the drop (50 \rightarrow 10%) in helical content at pH 9.5 \rightarrow 10.9 may result from the His deprotonation, thereby weakening the binding. At pH 4–8, the loss of α -helix within residues 1–9 could result from the negatively charged Asp1, Glu3, and Asp7 side chains, which hinder binding to the SDS. Similar findings were noticed with β -endorphin and somatostatin, in which α -helical structure is promoted in acidic SDS solution due to protonation of the negatively charged carboxylate side chains.⁶³

Additional support for the importance of electrostatic interactions in promoting the α -helix is seen in DTAC solution, in which there is a high α -helical content at pH 10.3 and small α -helical content at pH 3.4. The positively charged surfaces of the peptide and DTAC micelle oppose each other and prevent helix formation at pH 1–3, while at pH 9–12, the peptide becomes negatively charged and thus binds favorably to the DTAC.

In stark contrast to the behavior in micelles, at midrange pH (4–7) in 60% TFE or water alone, the α -helix structures rapidly unfold or perhaps pack together to produce oligomeric β -sheet structures that eventually precipitate into amyloid-like deposits.^{8,9,11,18,36} Thus, while not encouraging folding into an α -helix at midrange pH, the DPC micelle prevents aggregation of the 1–28 region into a β -sheet structure. The reason for the lack of β -sheet structure in the 1–28 region may result from the absence of the 29–40 or 29–42 hydrophobic regions, which are needed to induce an α -helix \rightarrow β -sheet conversion (discussed below).

Additional differences in the stabilities of the two α -helical segments (residues 2–7 and 10–28) take place with temperature. The NOESY data in SDS showed that both α -helices are stable up to 50 °C, while in 60% TFE and DPC, the smaller α -helix (residues 2–7) rapidly unfolds above 25 °C with the other helix (residues 10–28) unfolds above 35 °C (Figure 4). Further support for the thermal instability in DPC is shown by the NH temperature coefficients, in that all are relatively large (greater than 5), particularly within the His13–Ala21 region. From analysis of the 1D NMR data, it appears that both α -helices unfold to random coil or extended chain structures, but with cooling refold back to α -helices. By contrast, in SDS solution, the majority of the coefficients are less than 5, which suggests that most of the amides are solvent shielded and involved in relatively strong intrahelical NH hydrogen bonding. The lower coefficients in SDS is supported by the presence of NN($i,i+1$) NOESY connectivities at 50 °C, which are absent

(53) Halverson, K.; Fraser, P. E.; Kirschner, D. A.; Lansbury, P. T. *Biochemistry* **1990**, *29*, 2639–2644.

(54) Kelly, J. W.; Lansbury, P. T. *Amyloid* **1994**, *1*, 186–205.

(55) Snyder, S. W.; Lador, U. S.; Wade, W. S.; Wang, G. T.; Barrett, L. W.; Matayoshi, E. D.; Huffaker, H. J.; Krafft, G. A.; Holzman, T. F. *Biophys. J.* **1994**, *67*, 1216–1228.

(56) Shen, C.-L.; Murphy, R. M. *Biophys. J.* **1995**, *69*, 640–651.

(57) Soto, C.; Castano, E. M.; Frangione, B.; Inestrosa, N. C. *J. Biol. Chem.* **1995**, *270*, 3063–3067.

(58) Wood, S. J.; MacKenzie, L.; Maleef, B.; Hurler, M. R.; Wetzell, R. *J. Biol. Chem.* **1996**, *271*, 4086–4092.

(59) Kaneko, I.; Tutumi, S. *J. Neurochem.* **1997**, *68*, 438–439.

(60) Rizo, J.; Blanco, F. J.; Kobe, B.; Bruch, M. D.; Gierasch, L. M. *Biochemistry* **1993**, *32*, 4881–4894.

(61) Cantor, C. R.; Schimmel, P. R. *Biophysical Chemistry: Part I, The Conformation of Biological Macromolecules*; W. H. Freeman: New York, 1980.

(62) Shoemaker, K. R.; Kim, P. S.; York, E. J.; Stewart, J. M.; Baldwin, R. L. *Nature* **1987**, *326*, 563–567.

(63) Wu, C.-S. C.; Ikeda, K.; Yang, J. T. *Biochemistry* **1981**, *20*, 566–570.

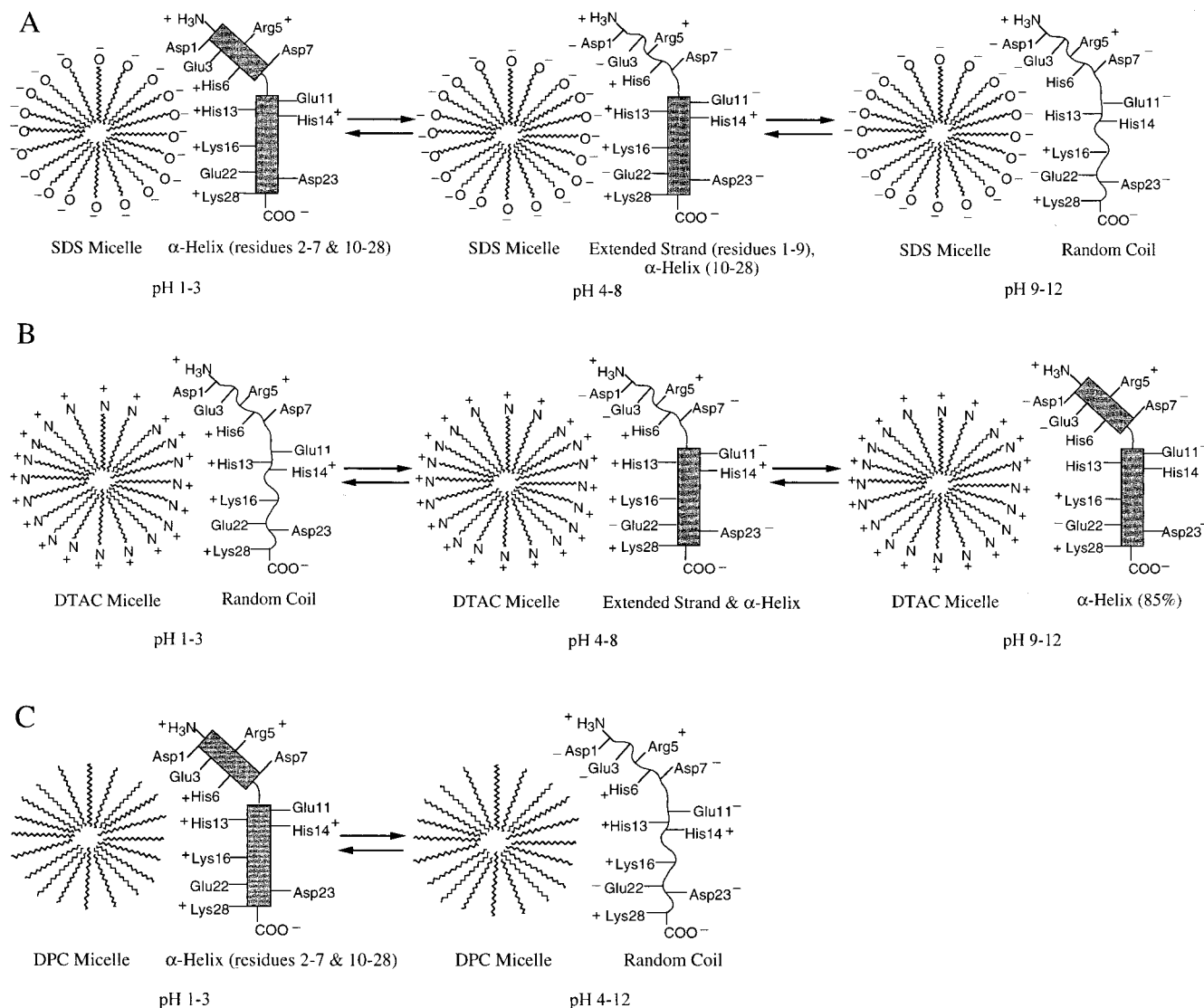


Figure 6. Structures and proposed interactions of the β -(1–28) peptide with the SDS, DPC, and DTAC micelles (A, B, and C, respectively) at pHs 1–3, 4–8, and 9–12. The micelles and amino acid side chains are drawn (not according to their relative sizes) with their expected charges at the three pH ranges. The α -helices are depicted with darkened cylinders, while the random coil or extended strand regions are drawn with wavy lines. The side chains of Asp1, Glu3, Asp7, Glu11, Glu22, and Asp23 are expected to deprotonate ($\text{COOH} \rightarrow \text{COO}^-$) above pH 4, and the side chains of His6, His13, and His14 should deprotonate ($3\text{NH}^+ \rightarrow 3\text{N}$) above pH 8. This mechanism emphasizes that the random coil and α -helical structures are in equilibrium throughout the entire pH range and that the electrostatic interactions between the charged side chains and the micelle surface stabilize the α -helix. The location of the peptide at the micelle surface, rather than the hydrophobic interior, is consistent with the NMR data (see text). The helical regions in SDS and DPC are supported by the NMR data, including the tertiary structure seen at low pH in 60% TFE³⁵ that had two α -helical regions (residues 2–7 and 10–28).^{35,52} The α -helical and random coil regions in DTAC were inferred from comparison of the CD data in DTAC with those in SDS and DPC.

in both 60% TFE and DPC solutions. For α -helices, amide-NH hydrogen bonds are present between the carbonyl oxygen of residue i and the NH of residue $i+4$. In 60% TFE, DPC, and SDS, there are higher coefficients within the Phe19–Phe20–Ala21–Glu22 region, suggesting that some weakening of the α -helix occurs between these amides and the carbonyl oxygens at Gln15–Lys16–Leu17–Val18. The most stable helical region is located between Tyr10 and Leu17, since the NH coefficients within the His13–His14–Gln15–Lys16–Leu17 stretch are comparatively low.

In summary, the CD and NOESY data taken at different pH and temperatures, as well as the profile of temperature coefficients, demonstrate that the SDS micelle confers greater stability to the α -helical structure.

Location of the Peptide about the Micelle. Several observations from the present data suggest that the entire length

of the β -(1–28) peptide associates at the membrane surface, rather than within the hydrophobic core of the SDS and DPC micelles. First, the amide temperature coefficients have a somewhat irregular pattern, indicating that the backbone amides are located at the lipid/water interface of the micelle. If a peptide segment were located in the hydrophobic interior of the micelle, then a long stretch of coefficients less than 5 should be observed. This pattern was seen for the β -(25–35) peptide in SDS, where the C-terminal Ile32–Met35 segment had reduced coefficients relative to the N-terminal region.⁶⁴ Second, recent work from our laboratory showed that the His side chains have elevated pK_a values in SDS solution, which is indicative of strong electrostatic binding to the negatively charged sulfate groups at the micelle surface (Clancy and Zagorski, unpub-

(64) Kohno, T.; Kobayashi, K.; Maeda, T.; Sato, K.; Takashima, A. *Biochemistry* **1996**, *35*, 16094–16104.

lished). Third, the line widths of the NMR resonances are smaller than would be expected for a β -(1–28)/micelle complex that would be approximately 15 kDa.³³ The narrower line widths are indicative of conformational mobility at the micelle surface. For example, differences were seen with the bacteriophage M13 coat protein, in that significantly narrower line widths were found for residues at the micelle surface compared to residues located in the central rigid micelle spanning α -helix.⁶⁵ Fourth, the observed variation in structure with both pH and the micelle head group charge indicates a high degree of peptide flexibility, which makes an internal micelle location highly unlikely. Fifth, the CD and NMR data were unaffected by changes in the micelle/peptide concentration ratios. This fact, together with the knowledge that the α -helical structure forms below the point where there is one molecule of micelle per molecule of peptide (on average, 56 and 63 monomers of DPC and SDS per micelle, respectively),³³ establishes that the α -helix structure is probably stabilized by rapid exchange among the micelle surfaces. Finally, the location of the β -(1–28) at the micelle surface is consistent with its location in the precursor protein APP, in which the 1–28 region is located in the extracellular domain while the 29–42 region is imbedded in the transmembrane domain.

Comparison of the Micelle-Bound β -(1–28) Structures with Previous Studies. For the β -peptide, the solution conditions greatly influence the relative proportions and types of structures (α -helix, β -sheet, or random coil). Some of these variables include the peptide length [i.e., the β -(1–40) is less likely to form aggregated β -sheet than the β -(1–42)], peptide concentration, starting peptide aggregation state, pH, solvent hydrophobicity, trace metals, and ionic strength.^{9–11,18,55,66} This extreme sensitivity of structure and aggregation state to the solution conditions has greatly complicated biophysical data interpretations.

Due to its instability and susceptibility to aggregation, only a limited number of solution NMR studies have been reported with the β -peptide. It is important to recognize that these studies used different solvent conditions and different peptides, so the structures often show some variations. In previous work, we showed that the three-dimensional structure of the β -(1–28) below pH 3 in 60% TFE was completely α -helical.³⁵ At pH 3–4, the first nine, N-terminal residues unfold, leaving an α -helix at Tyr10–Lys28. Because the α H chemical shifts and NOESY data are nearly identical in 60% TFE, SDS, and DPC, similar α -helical backbone structures probably exist at acidic pH. By comparison, related NMR studies carried out in water alone below pH 4 and above pH 7 indicate the structure of β -(1–28) is essentially random coil.^{43,52} This establishes that the α -helical structure requires a membrane mimetic environment.

The NMR-derived tertiary structure for the β -(1–40) peptide in 30% TFE solution reportedly contained two well-defined α -helices at Gln15–Asp23 and Ile31–Met35.⁶⁷ In contrast, the NMR-derived three-dimensional structure for the β -(25–35) peptide was completely α -helical in SDS solution, with the N-terminal region exposed to solvent and the C-terminal region located in the hydrophobic interior.⁶⁴ Other NMR studies of a β -(10–35)-CONH₂ fragment demonstrated a turn–strand–turn

motif between His13 and Val24 in water solution.⁴³ By contrast, related CD and NMR studies of a β -(12–28) fragment established that a shorter Gln15–Lys28 segment becomes α -helical in SDS solution.⁶⁸ The reason for the shorter helix in the latter study may result from the absence of Glu11, which above pH 4 interacts favorably with the positively charged N-terminus of the α -helix macrodipole.⁵² This latter study also found that the interaction of the β -(12–28) with DPC was weak, but sufficient to promote partial α -helical structure below pH 4, which is consistent with the present studies of the β -(1–28).

Numerous biophysical studies using techniques other than NMR have already explored β -peptide membrane interactions.^{58,64,66,68–73} A few discrepancies exist among these studies, which in part can be explained by differences in the initial aggregation states and structures of the β -peptides.^{74,75} Some studies showed that the β -sheet is a predominate structural motif on the membrane surface, which may or may not become partly imbedded into the membrane. As mentioned before, the β -sheet structure is neurotoxic and aggregated and eventually precipitates as an amyloid plaque.^{30,31} It was also found that some lipids do not promote β -sheet structure,⁷³ including micelles⁵⁸ and neutral lipid vesicles in which the β -(1–40) peptide formed random coil structure at physiological pH.⁶⁶ Both of these results agree with the present work with the β -(1–28) in neutral DPC micelles. On the other hand, it was also reported that negatively charged lipid vesicles promote β -sheet structure, presumably by either random coil \rightarrow β -sheet or α -helix \rightarrow β -sheet conversions.^{66,76}

In light of the above results and those of the present study, one possible outcome is that the α -helix may represent an early folded intermediate in the 1–28 region and that the 29–40 or 29–42 hydrophobic region promotes an α -helix \rightarrow β -sheet conversion for the complete peptide. In fact, most membrane-associating peptides produce α -helices on biological membrane surfaces.³³ A reasonable mechanism could involve the charged 1–28 region first contacting the membrane surface and producing monomeric α -helical structure, which later rearranges (α -helix \rightarrow β -sheet) after the 29–40 or 29–42 region comes in contact with the membrane.³⁶ This idea is consistent with the different structures seen in the 1–24 region in both monomeric and aggregated β -(1–40) peptide.⁷⁷ Once formed, the β -sheet structure would continue to aggregate, bind more effectively to the membrane surface,⁷⁸ and promote toxicity, perhaps by generating its own micelle-like structure on the membrane surface that penetrates and disrupts the membrane.^{70,71,79,80}

(68) Sticht, H.; Bayer, P.; Willbold, D.; Dames, S.; Hilbich, C.; Beyreuther, K.; Frank, R. W.; Rösch, P. *Eur. J. Biochem.* **1995**, *233*, 293–298.

(69) Fletcher, T. G.; Keire, D. A. *Protein Sci.* **1997**, *6*, 666–675.

(70) Fabian, H.; Szendrei, G. I.; Mantsch, H. H.; Greenberg, B. D.; Ötvös, L. *Eur. J. Biochem.* **1994**, *221*, 959–964.

(71) McLaurin, J.; Chakrabarty, A. *J. Biol. Chem.* **1996**, *271*, 26482–26489.

(72) Pillot, T.; Marc, G.; Vanloo, B.; Talussot, C.; Brasseur, R.; Vandekerckhove, J.; Rosseneu, M.; Lins, L. *J. Biol. Chem.* **1996**, *271*, 28757–28765.

(73) Choo-Smith, L.-P. i.; Surewicz, W. K. *FEBS Lett.* **1997**, *402*, 95–98.

(74) Klunk, W. E.; Xu, C.-J.; McClure, R. J.; Panchalingam, K.; Stanley, J. A.; Pettegrew, J. W. *J. Neurochem.* **1997**, *69*, 266–272.

(75) Soto, C.; Castaño, E. M.; Kumar, R. A.; Beavis, R. C.; Frangione, B. *Neurosci. Lett.* **1995**, *200*, 105–108.

(76) Jao, S.-C.; Ma, K.; Talafous, J.; Orlando, R.; Zagorski, M. G. *Amyloid* **1997**, *4*, 239–252.

(77) Seelig, J.; Lehmann, R.; Terzi, E. *Mol. Membr. Biol.* **1995**, *12*, 51–57.

(78) Kametani, F.; Tanaka, K.; Tokuda, T.; Allsop, D. *Brain Res.* **1995**, *703*, 237–241.

(65) Van Den Hooven, H. W.; Spronk, C. A. E. M.; Van De Kamp, M.; Konings, R. N. H.; Hilbers, C. W.; Van De Ven, F. J. M. *Eur. J. Biochem.* **1996**, *235*, 394–403.

(66) van de Ven, F. J. M.; van Os, J. W. M.; Aelen, J. M. A.; Wymenga, S. S.; Remerowski, M. L.; Konings, R. N. H.; Hilbers, C. W. *Biochemistry* **1993**, *32*, 8322–8328.

(67) Terzi, E.; Hölzemann, G.; Seelig, J. *J. Mol. Biol.* **1995**, *252*, 633–642.

Related α -helix \rightarrow β -sheet conversions for other peptides and proteins,^{81–87} including peptide segments of the prion proteins,^{41,88} are well documented. In addition, local alterations of lipid compositions at the site of β -peptide binding could alter the charge at the membrane surface and perhaps trigger the α -helix \rightarrow β -sheet rearrangement resulting in amyloid deposition.

Biological Implications. The interaction of the β -(1–28) peptide with micelles suggests a preferential binding between the β -peptide and negatively charged biological membranes. As mentioned before, the SDS and DPC micelles readily mimic biological membrane interfaces and also the lipid environments of lipoproteins.⁸⁹ Upon interaction with a naturally, charged membrane, the β -(1–28) peptide region would be expected to initially adopt α -helical structure that does not insert into the hydrocarbon interior. This situation may occur during circulation in human plasma when the β -peptide becomes bound to lipoproteins, albumin, Apo-J, or TTR.^{20,24,90} Significantly, the binding to lipoproteins decreases the toxicity in cortical cell culture studies, which indirectly suggests the bound structure is α -helix since the β -sheet structure is toxic.^{91,92}

Recent studies using synchrotron FTIR microspectroscopy showed that the β -peptide adopts significant quantities of α -helical structure in the brain gray matter.⁹³ In addition, it is thought that the β -peptide cytotoxicity is mediated by its association at the membrane surface of neurons.^{1,31,94,95} Previous work showed that the β -(1–28) peptide is not toxic to neurons⁹⁶ and that the β -(1–42) but not the β -(1–28) is accumulated intracellularly.⁹⁷ The explanation was that the β -(1–28) is too polar and requires the hydrophobic 29–42 region to insert into the membrane. Thus, for some brain microenvironmental conditions, the 1–28 region may remain as a nontoxic, α -helix on the membrane surface of cells, but once the 29–42 region inserts into the membrane, an α -helix \rightarrow β -sheet conversion may occur inducing toxicity and cell death. Additional studies to investigate these possibilities are currently underway.

(79) Soreghan, B.; Kosmoski, J.; Glabe, C. *J. Biol. Chem.* **1994**, *269*, 28551–28554.

(80) Lomakin, A.; Chung, D. S.; Benedek, G. B.; Kirschner, D. A.; Teplow, D. B. *Proc. Natl. Acad. Sci.* **1996**, *93*, 1125–1129.

(81) Batenburgh, A. M.; Brasseur, R.; Ruyschaert, J.-M.; van Scharrenburgh, G. J. M.; Slotboom, A. J.; Demel, R. A.; Kruijff, B. *J. Biol. Chem.* **1988**, *263*, 4202–4207.

(82) Dunker, A. K.; Fodor, S. P. A.; Williams, R. W. *Biophys. J.* **1982**, *37*, 201–203.

(83) Verlinde, C. L.; Hol, W. G. *Structure* **1994**, *2*, 577–587.

(84) Fan, P.; Bracken, C.; Baum, J. *Biochemistry* **1993**, *32*, 1573–1582.

(85) Li, Z.; Glibowicka, M.; Joensson, C.; Deber, C. M. *J. Biol. Chem.* **1993**, *268*, 4584–4587.

(86) Graf v. Stosch, A.; Jiménez, M. A.; Kinzel, V.; Reed, J. *Proteins: Struct., Funct., Genet.* **1995**, *23*, 196–203.

(87) Zhang, S.; Rich, A. *Proc. Natl. Acad. Sci. U.S.A.* **1997**, *94*, 23–28.

(88) Nguyen, J.; Baldwin, M. A.; Cohen, F. E.; Prusiner, S. B. *Biochemistry* **1995**, *34*, 4186–4192.

(89) Wang, G.; Pierens, G. K.; Treleaven, W. D.; Sparrow, J. T.; Cushley, R. J. *Biochemistry* **1996**, *35*, 10358–10366.

(90) Matsubara, E.; Frangione, B.; Ghiso, J. *J. Biol. Chem.* **1995**, *270*, 7563–7567.

(91) Farhangrazi, Z. S.; Ying, H.; Bu, G.; Dugan, L. L.; Fagan, A. M.; Choi, D. W.; Holtzman, D. M. *NeuroReport* **1997**, *8*, 1127–1130.

(92) Hertel, C.; Terzi, E.; Hauser, N.; Jakob-Rötne, R.; Seelig, J.; Kemp, J. A. *Proc. Natl. Acad. Sci. U.S.A.* **1997**, *94*, 9412–9416.

(93) Choo, L.-P. i.; Wetzel, D. L.; Halliday, W. C.; Jackson, M.; LeVine, S. M.; Mantsch, H. H. *Biophys. J.* **1996**, *71*, 1672–1679.

(94) Mattson, M. P.; Barger, S. W.; Cheng, B.; Lieberburg, I.; Smith-Swintosky, V. L.; Rydel, R. E. *Trends Neurosci.* **1993**, *16*, 409–414.

(95) Cribbs, D. H.; Pike, C. J.; Weinstein, S. L.; Velazquez, P.; Cotman, C. W. *J. Biol. Chem.* **1997**, *272*, 7431–7436.

(96) Pike, C. J.; Burdick, D.; Walencewicz, A. J.; Glabe, C. G.; Cotman, C. W. *J. Neurosci.* **1993**, *13*, 1676–1687.

(97) Yang, A. J.; Knauer, M.; Burdick, D. A.; Glabe, C. *J. Biol. Chem.* **1995**, *270*, 14786–14792.

Conclusion

The present study established that different lipid environments can modulate the structure of the β -(1–28) peptide. The micelles are simple model systems that may mimic the binding between the β -peptide and lipid environments in vivo. The present data suggest that a charged lipid surface is required to promote the α -helical structure, suggesting that electrostatic interactions between the 1–28 peptide region and the lipid/water interface of a biological membrane are important. The 1–28 region does not become imbedded into the interior of micelle, and the specific residues that might be involved in this electrostatic interaction have yet to be identified.

We believe that the α -helical structure is an appropriate target for the design of amyloid inhibitors. The α -helical structure is monomeric and stable, thus suitable for modern structure-based drug design methods.⁸³ These results suggest that biological macromolecules with a positively or negatively charged surface are essential for stabilization of the α -helical structure. Such stabilization may be critical to preventing an α -helix (soluble, monomeric) \rightarrow β -sheet (insoluble amyloid deposit, toxic) conformational transition from occurring in the brains of AD patients.

Experimental Section

Peptide Synthesis and Purification. The β -(1–28) peptide was synthesized, purified, and characterized as described previously.¹⁸ Purification was done in two steps: (1) trituration by washing repeatedly with diethyl ether, followed by (2) reverse-phase HPLC with a C₄ column (Cosmacil 5C₄-300 or Vydac 214TP510) and a linear gradient of 20–80% acetonitrile and 0.1–0.08% trifluoroacetic acid in water. Peptide identity was verified by amino acid analysis, fast-atom bombardment mass spectrometry, and ¹H NMR spectroscopy, which together showed a purity level of approximately 95%.⁷⁶

CD Studies. Samples for CD spectroscopy were prepared by dissolving the β -(1–28) peptide (1.8 mg, 0.5 μ mol, 250 μ M) in distilled water (2.0 mL) that contained the sodium salts of the micelles SDS, DPC, or DTAC at 20 or 75 mM concentrations. For the DTAC solutions, aliquots (1.0 mL) from a commercial stock solution (Pfaltz & Bauer, Inc.) in 2-propanol–water were dried and weighed under N₂, then dissolved in a precise volume of distilled water to provide 20 or 75 mM solutions. To provide an accurate concentration value of the commercial DTAC solution, the first part of the experiment was performed separately in triplicate.

The CD spectra were obtained at room temperature with a Jasco spectropolarimeter (Model J-600A). Unless otherwise noted, a quartz cell (Hellma, Inc.) of 0.01-cm path length was used to obtain spectra at 1-nm intervals from 190 to 260 nm. Spectra resulted from averaging eight scans, followed by analysis with the Jasco J-600 program that was located on the DP-501 computer of the spectropolarimeter. The CD spectra of the SDS, DPC, and DTAC micelle solutions showed no absorptions and, therefore, were not subtracted from the spectra containing peptide. Measurements with extra salt were not undertaken, since prior studies showed that salts such as NaCl have little effect on the binding of the β -peptide to either rat cortical homogenates (lipids and membrane-associated proteins) or artificial neuronal membranes (lipids only).⁴³

For the pH studies, two peptide–micelle solutions were prepared at low and high pH. This procedure avoided possible structure perturbations that could occur over time (aging), as previously seen in water or 60% TFE at midrange pH 4–7.^{8,9,11} As it happened, no time-dependent variations were apparent in the present study which was done in micelle solutions. The β -(1–28) peptide–micelle solution (2 mL) was split into two equal parts, after which the pH was adjusted to approximately 2–3 and 10–12 for each solution. The CD spectra were recorded within 10 min after the pH adjustment, and thereafter, the pH was increased or decreased for the low- and high-pH solutions, respectively. The pH values were measured with a pH meter (Model PHB-62, Omega Engineering, Inc.) equipped with an electrode (Model

MI-412, Microelectrodes, Inc.) that was calibrated with pH 4.00, 7.00, and 12.00 buffers. The CD data were converted to θ values (deg cm² dmol⁻¹) using the β -(1–28) concentration and the number of amino acid residues. The percent α -helix was obtained by comparing the ratios of the θ values at 195 and 208 nm to the NMR data. Using the NMR data to establish a reference state for α -helicity below pH 3 (Figure 4), the ratio of the CD bands in SDS and DPC solution were standardized to 85% α -helix (Table 1). Similar procedures, using a combination of NMR and ratios of CD bands, have been utilized to obtain reliable estimates of secondary structures for other peptides.^{98–100}

NMR Studies. Perdeuterated SDS-*d*₂₅ and DPC-*d*₃₈ as well as the solvent D₂O were obtained from Cambridge Isotopes, Inc. (Andover, MA). Two samples were prepared for the 2D NMR measurements in a mixture by volume (9:1) of H₂O:D₂O: (1) one sample containing 3.6 mg (0.001 mmol) of the β -(1–28) peptide in a solution (0.50 mL) of SDS-*d*₂₅ (450 mM) and (2) the other sample containing 2.6 mg (0.0007 mmol) of the β -(1–28) peptide in a solution (0.50 mL) of DPC-*d*₃₈ (120 mM). For the diffusion coefficient measurements, two β -(1–28) samples (2.0 mM and 0.20 mM) were prepared in D₂O solution (0.50 mL) with 150 mM SDS-*d*₂₅ at pH 3.0. All solutions contained 0.5 mM Na₂EDTA and 0.05 mM NaN₃. The pHs of the solutions were adjusted with a pH meter (Corning 340) equipped with an pH electrode that fit inside the NMR tube. The desired pH values were obtained at room temperature by adding microliter amounts of dilute HCl or NaOH and were not corrected for isotope effects.

All NMR spectra were acquired at 500 or 600 MHz using a General Electric GN-500 or Varian Inova-600 spectrometer. The NMR data were transferred to Indigo XS24 (Silicon Graphics, Inc.) computer workstations and processed using the Felix program (version 95, Biosym, Inc.). Chemical shifts were referenced to an internal standard of sodium 3-(trimethylsilyl)propionate-2,2,3,3-*d*₄ (TSP), and probe temperatures were calibrated using neat methanol.¹⁰¹

The diffusion coefficients (*D*) were obtained using the PFG–water–sLED (longitudinal eddy–current delay) pulse sequence.⁴⁵ The maximum magnitude of the gradient was calibrated with a profile experiment, which was 32 G/cm for a 5-mm indirect detection probe equipped with an actively shielded *z*-gradient coil. Data accumulation involved acquiring an array of 15 spectra (32 scans each, 5-s recycle delay) with different gradient strengths (*g*) varying from 0.3 to 30 G/cm. The NMR signal intensities are related to the *D* according to the following relationship:

$$R = \exp[(-\gamma g \delta)^2 D (\Delta - \delta/3)]$$

where *R* is the ratio of intensities for a resonance with the gradient turned on (*I*) to that with the gradient turned off (*I*₀), γ is the gyromagnetic ratio of ¹H (2.675 × 10⁴ G⁻¹ s⁻¹), *g* and δ are the magnitude and duration of the gradient pulse, respectively, and Δ is the time between the gradient pulses. For our studies, the following parameters were used: $\delta = 5.5$ ms, *g* = 0.3–30 G/cm, $\Delta = 220$ –320 ms, and a longitudinal eddy–current delay of 40 ms. The upfield methyl signals (0.73–1.52 ppm) and downfield aromatic signals (6.74–8.66 ppm) were integrated to provide the signal intensities (*I* and *I*₀), and these data were approximated as single, exponentially decaying curves [plots of *R* vs (*g*²)] using averaged fitting values (Origin program, version 4.0, Microcal, Inc.).

To check the accuracy of our diffusion measurements, we determined the *D* values for lysozyme and ubiquitin, which are two well-

(98) Bradley, E. K.; Thomason, J. F.; Cohen, F. E.; Kosen, P. A.; Kuntz, I. D. *J. Mol. Biol.* **1990**, *215*, 607–622.

(99) Merutka, G.; Morikis, D.; Brüttschweiler, R.; Wright, P. E. *Biochemistry* **1993**, *32*, 13089–13097.

(100) Muñoz, V.; Blanco, F. J.; Serrano, L. *Protein Sci.* **1995**, *4*, 1577–1586.

(101) Van Geet, A. L. *Anal. Chem.* **1970**, *42*, 679–680.

characterized protein systems. For these proteins, our *D* values were almost in complete agreement ($\pm 0.02 \times 10^{-6}$ cm² s⁻¹) with the literature values,⁴⁵ hence establishing the validity in our experimental approach. The *D* for the β -(1–28) were measured in triplicate and at two different peptide concentrations (2.0 and 0.20 mM) in 150 mM SDS-*d*₂₅ solution at pH 3.0; the calculated *D* values were 6.1×10^{-7} and 6.3×10^{-7} cm² s⁻¹ ($\pm 0.24 \times 10^{-7}$ cm² s⁻¹), respectively. The effect of the micelle on the overall *D* was addressed by measuring *D* for a peptide-free SDS-*d*₂₅ solution (150 mM); this was $4.2 (\pm 0.24) \times 10^{-7}$ cm² s⁻¹. This latter value took into account the presence of small amounts of free (nonmicellar) detergent molecules, according to the following relationship: $D = (D_{\text{obs}} - [\text{cmc}]/[\text{total detergent concentration}] \times D_{\text{free}})/(1 - [\text{cmc}]/[\text{total detergent concentration}])$, where cmc corresponds to the critical micelle concentration, *D*_{obs} is the observed diffusion coefficient, and *D*_{free} is the diffusion coefficient for free detergent molecules (measured at submicellar total detergent concentration).¹⁰²

Two-dimensional nuclear Overhauser enhancement spectroscopy (NOESY)¹⁰³ and total correlation spectroscopy (TOCSY)^{104,105} were run in the phase-sensitive mode with quadrature detection in both dimensions. Mixing times of 150–250 and 30–80 ms were employed in the NOESY and TOCSY, respectively. The total recycle delay between scans was approximately 1.5–2.0 s, which included the acquisition and mixing times. For the determination of the NH temperature coefficients, the chemical shifts of the amide-NH protons were obtained from NOESY or TOCSY spectra acquired at 15.0, 20.0, 25.0, 30.0, 35.0, 40.0, and 50.0 °C. The temperature coefficients ($-\Delta\delta/\Delta T$, ppb) were taken as the slopes from a least-squares computer-fitted lines of the chemical shifts against temperature. A more complete description of the NMR acquisition and processing parameters can be found in the Supporting Information.

Acknowledgment. Supported in part by grants from the American Health Assistance Foundation, the American Federation of Aging Research, the Suntory Institute for Bioorganic Research, the Smokeless Tobacco Research Council, the National Institutes of Aging (AG-08992-06 and AG-14363-01), a Claire Boothe Luce Graduate Fellowship to E.L.C., and a Faculty Scholars Award from the Alzheimer's Association to M.G.Z. (FSA-94-040). The 600-MHz NMR spectrometer was purchased with funds provided by the National Science Foundation, the National Institutes of Health, and the State of Ohio. We thank Mark Smith, Kan Ma, Chaim Sukenik, Olga Vinogradova, Frank Sönnichsen, Chuck Sanders, Larry Sayre, Anita Hong (Anaspec, Inc.), and Witold Surewicz for helpful discussions.

Supporting Information Available: A complete contour plot of the NOESY spectrum for the β -(1–28) in DPC-*d*₃₈ and more information about the parameters for processing of the NMR data (4 pages, print/PDF). See any current masthead page for ordering information and Web access instructions.

JA9738687

(102) Vinogradova, O.; Sönnichsen, F.; Sanders, C. R. *J. Biomol. NMR* **1998**, *4*, 381–386.

(103) Kumar, A.; Ernst, R. R.; Wüthrich, K. *Biochem. Biophys. Res. Commun.* **1980**, *95*, 1–6.

(104) Bax, A.; Davis, D. G. *J. Magn. Reson.* **1985**, *65*, 355–360.

(105) Rance, M. *J. Magn. Reson.* **1987**, *74*, 557–564.

(106) States, D. J.; Haberkorn, R. A.; Ruben, D. J. *J. Magn. Reson.* **1982**, *48*, 286–292.

(107) Otting, G.; Widmer, H.; Wagner, G.; Wüthrich, K. *J. Magn. Reson.* **1986**, *66*, 187–193.

(108) Güntert, P.; Wüthrich, K. *J. Magn. Reson.* **1992**, *96*, 403–407.